Eco de Loschmidt en cadenas con frustración

Contenidos

01 Paper

Presentación del trabajo

02 Eco de Loschmidt

Como la transformada de Fourier de la prob. de trabajo

03 Frustración topológica

En cadenas con interacción antiferro

04 Resultados

Distinto comportamiento para N par o impar incluso en el límite termodinámico

05 Conclusiones e ideas a futuro

Resumen de las ideas importantes

01

Paper

An odd thermodynamic limit for the Loschmidt echo

Gianpaolo Torre,[1] Vanja Marić,[2,3] Domagoj Kuić,[2] Fabio Franchini,[2] and Salvatore Marco Giampaolo[2]
[1] *Department of Physics, Faculty of Science, University of Zagreb, Bijenička cesta 32, 10000 Zagreb, Croatia.*
[2] *Ruder Bošković Institute, Bijenička cesta 54, 10000 Zagreb, Croatia*
[3] *SISSA and INFN, via Bonomea 265, 34136 Trieste, Italy*
(Dated: May 17, 2021)

¿Es posible distinguir un sistema compuesto por un número de Avogadro de partículas idénticas de uno con una partícula adicional?

Para ello es necesario un sistema que tenga observables sensibles al número de partículas

Para las cadenas antiferromagnéticas es posible tener "frustración" exclusivamente para N impar (para N par no existe tal frustración)

Esta rompe una simetría local y genera cambios en el espectro de energías detectables con el eco de Loschmidt

An odd thermodynamic limit for the Loschmidt echo

Gianpaolo Torre,[1] Vanja Marić,[2,3] Domagoj Kuić,[2] Fabio Franchini,[2] and Salvatore Marco Giampaolo[2]
[1] Department of Physics, Faculty of Science, University of Zagreb, Bijenička cesta 32, 10000 Zagreb, Croatia.
[2] Ruđer Bošković Institute, Bijenička cesta 54, 10000 Zagreb, Croatia
[3] SISSA and INFN, via Bonomea 265, 34136 Trieste, Italy
(Dated: May 17, 2021)

Cadena circular antiferro con CC periódicas (ID)

- N par → Ausencia de frustración
- N impar → Presencia de frustración

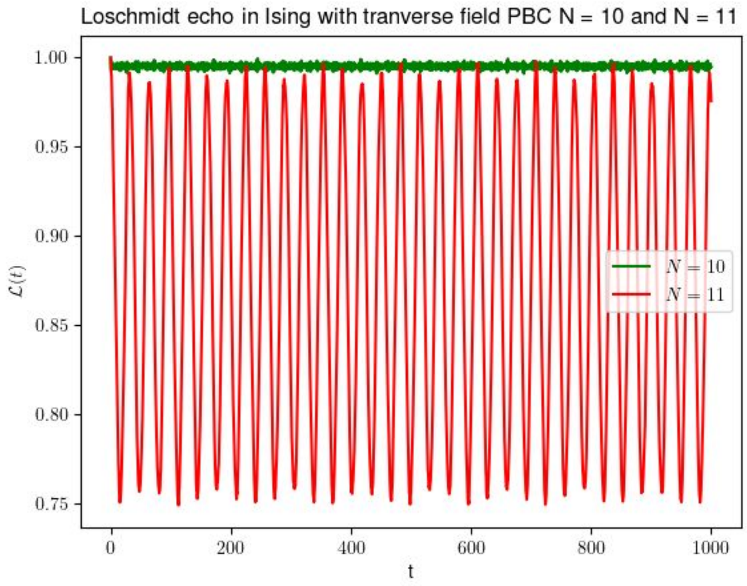

Cadena circular antiferro con CC periódicas

N impar

Presencia de frustración

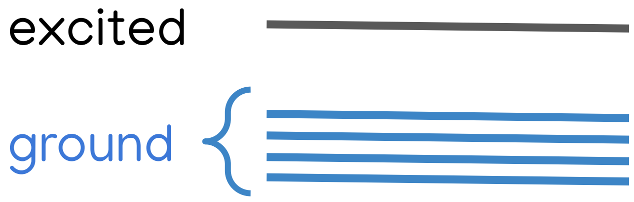

N par

Ausencia de frustración

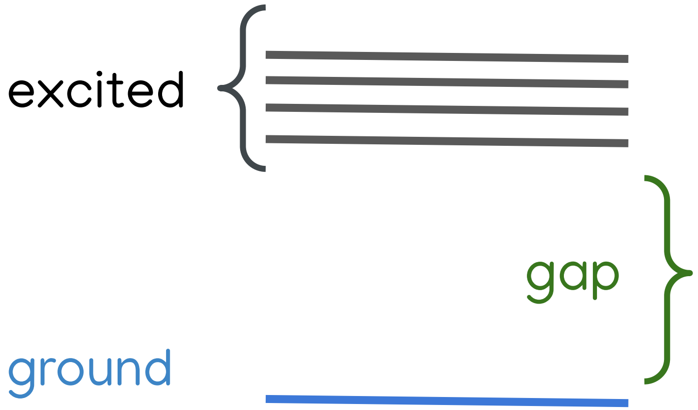

02

Eco de Loschmidt

Eco de Loschmidt $\mathcal{L}(t) = |\langle\psi_0|e^{iH_2t/\hbar}e^{-iH_1t/\hbar}|\psi_0\rangle|^2$

como medida de irreversibilidad

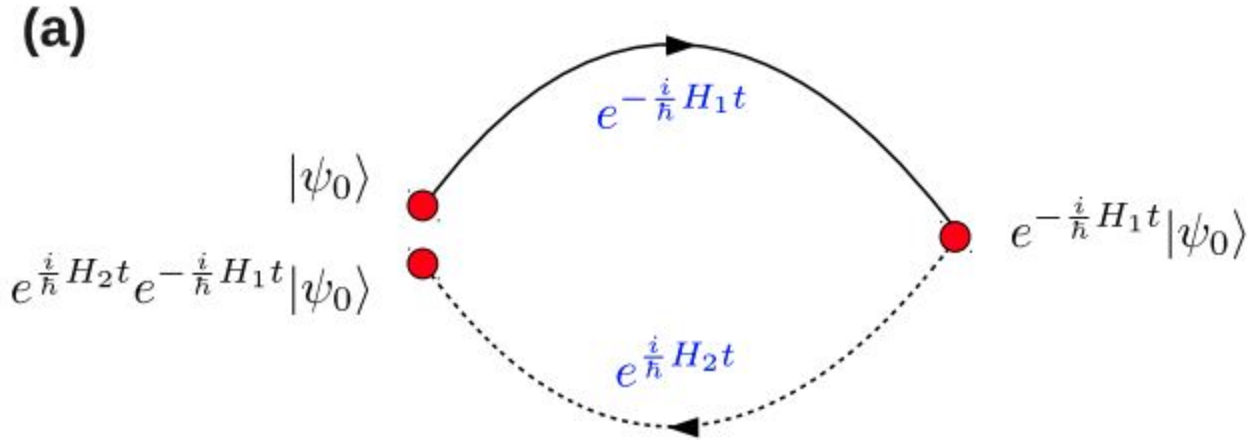

Goussev, A., Jalabert, R. A., Pastawski, H. M., & Wisniacki, D. (2012). Loschmidt echo. *arXiv preprint arXiv:1206.6348*.

Eco de Loschmidt $\mathcal{L}(t) = \left|\langle\psi_0|e^{iH_2t/\hbar}e^{-iH_1t/\hbar}|\psi_0\rangle\right|^2$

como medida de la sensibilidad de la evolución a perturbaciones

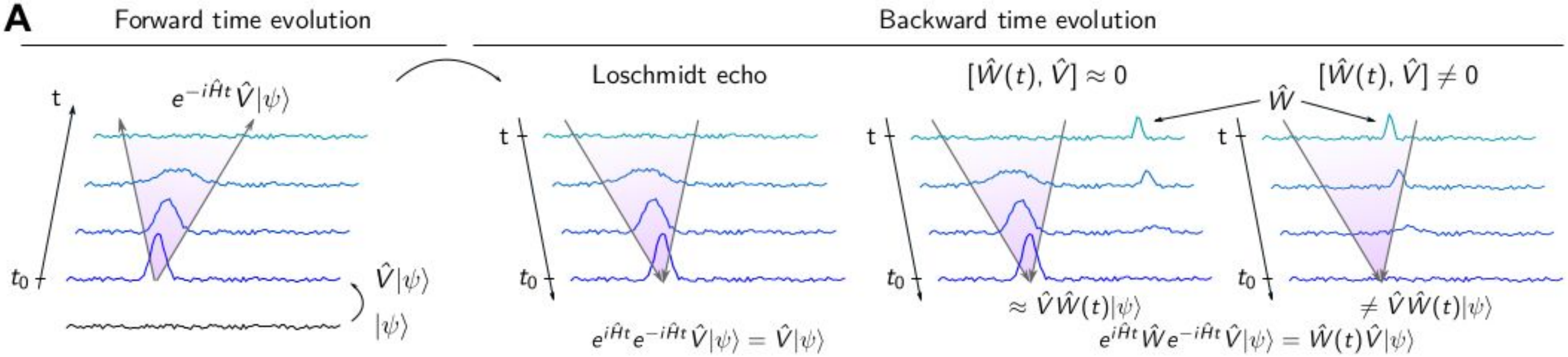

Braumüller, (2021). Probing quantum information propagation with out-of-time-ordered correlators. *arXiv preprint arXiv:2102.11751*.

Quench

$$H_0|g\rangle = E_0^{(0)}|g\rangle$$

$$H_1 = H_0 + \lambda H_p$$

$$H_1|n\rangle = E_n|n\rangle$$

Preparo al estado en un autoestado de H_0 y cambio repentinamente un parámetro del hamiltoniano (λ)

Ej: Ising con campo transverso + impureza

$$H_1 = H_0 + \lambda\,\sigma_N^z$$

$$H_0 = \sum_{j=1}^{N}\left(\sigma_j^x\sigma_{j+1}^x + h\sigma_j^z\right)$$

$$\lambda = 0 \xrightarrow{\text{Quench}} \lambda > 0$$

Eco de Loschmidt $\mathcal{L}(t)$

quench

$$H_0|g\rangle = E_0^{(0)}|g\rangle$$

$$H_1|n\rangle = E_n|n\rangle$$

$$H_1 = H_0 + \lambda H_p$$

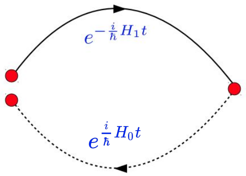

$$\mathcal{L}(t) = |\langle g|e^{iH_0 t}e^{-iH_1 t}|g\rangle|^2$$

$$\mathcal{L}(t) = |\langle g|e^{iE_0^0 t}e^{-iH_1 t}|g\rangle|^2$$

$$\mathcal{L}(t) = |\langle g|e^{-iH_1 t}|g\rangle|^2$$

$$\mathcal{L}(t) = \left|\sum_n e^{-iE_n t}|c_n|^2\right|^2, \qquad c_n = \langle n|g\rangle.$$

$$\hbar \equiv 1$$

Eco de Loschmidt

Haque, M. (2016). Overlap distributions for quantum quenches in the anisotropic Heisenberg chain. 013104.

quench

$$H_1 = H_0 + \lambda H_p$$

$$H_0 |g\rangle = E_0^{(0)} |g\rangle$$

$$H_1 |n\rangle = E_n |n\rangle$$

$$\mathcal{L}(t) = \left| \sum_n \mathrm{e}^{-\mathrm{i}E_n t} |c_n|^2 \right|^2 = \left| \int \frac{d\omega}{2\pi} p(\omega) \mathrm{e}^{-\mathrm{i}\omega t} \right|^2$$

Transformada de Fourier de la probabilidad de trabajo $p(w)$

$$p(w) = 2\pi \sum_n |c_n|^2 \delta(w - (E_n - E_i))$$

$$c_n = \langle n|g\rangle \, .$$

03

Frustración topológica

Sub-lattice symmetry

$$H_\Omega\left(0, J, \{S_i\}\right) = -J \sum_{<ij>} S_i S_j$$

$$H_\Omega\left(0, J, \left\{S_i^A\right\}, \left\{S_i^B\right\}\right) = -J \sum_{<ij>} S_i^A S_j^B$$

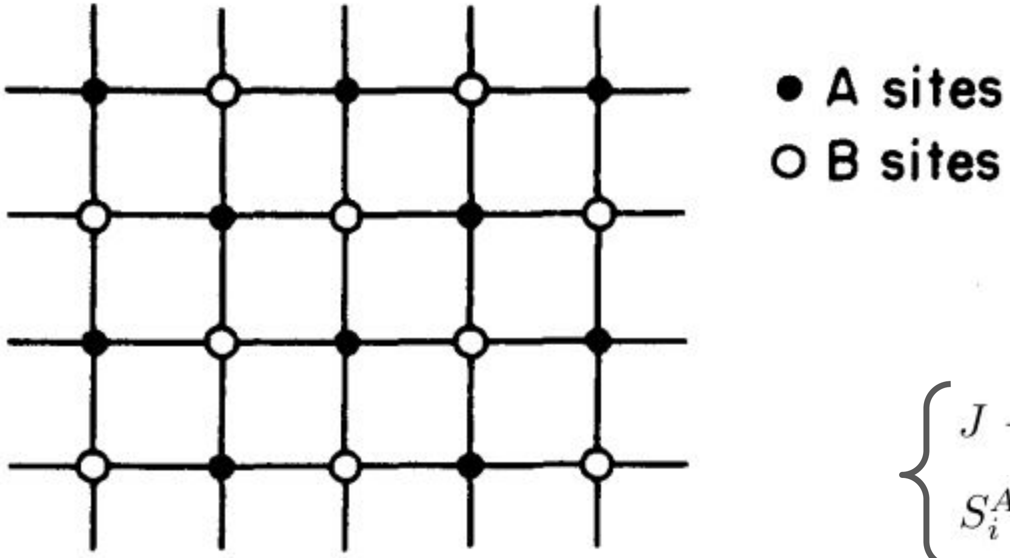

$$\begin{cases} J \to -J \\ S_i^A \to -S_i^A \end{cases}$$

es una simetría

Goldenfeld, N. (2018). *Lectures on phase transitions and the renormalization group*. CRC Press.

Balents, L. (2010). Spin liquids in frustrated magnets. *Nature*, *464*(7286), 199-208.

Frustración topológica
ejemplo sencillo

$$H = \sum_{j=1}^{N} \sigma_j^z \sigma_{j+1}^z$$

Interacción antiferromagnética:

La energía disminuye cuando "apareo" dos espines

$$\begin{cases} J \to -J \\ S_i^A \to -S_i^A \end{cases}$$

no es una simetría

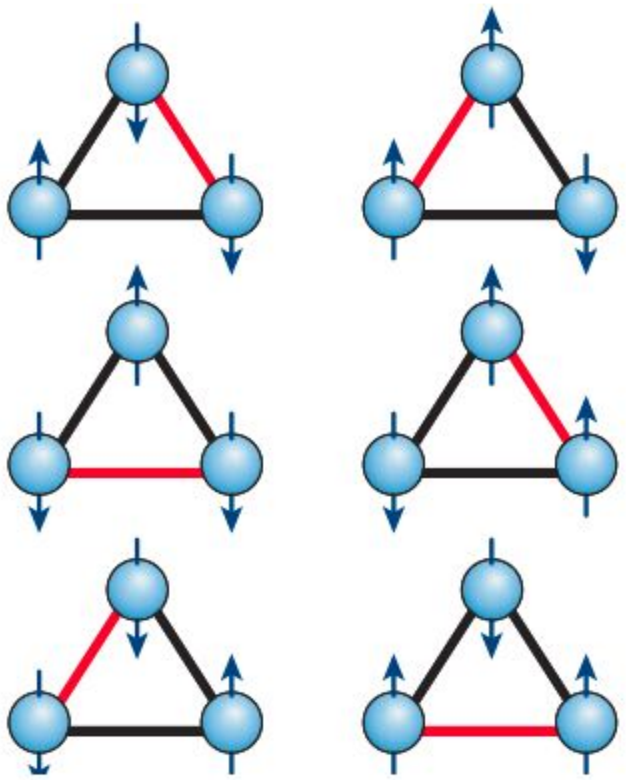

¡paso de 2 a 6 ground states!

Frustración topológica

sistema paper

$$H = \sum_{j=1}^{N} \sigma_j^z \sigma_{j+1}^z$$

Interacción antiferromagnética:

La energía disminuye cuando "apareo" dos espines

$$\begin{cases} J \to -J \\ S_i^A \to -S_i^A \end{cases}$$

no es una simetría para N impar

N=8

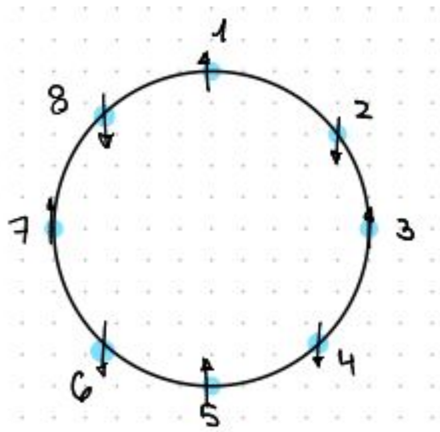

N=9

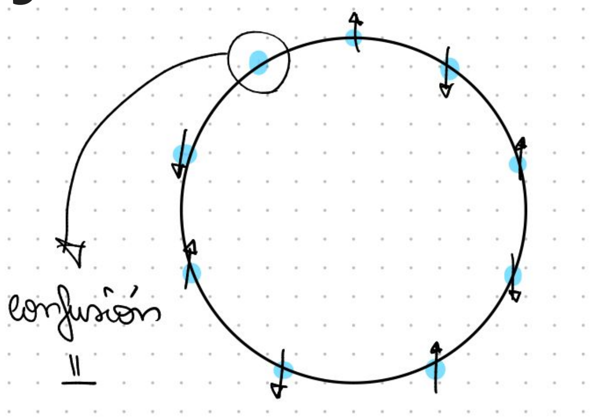

Consecuencias en el espectro

N impar

Presencia de frustración

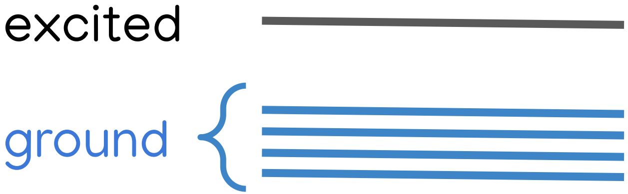

N par

Ausencia de frustración

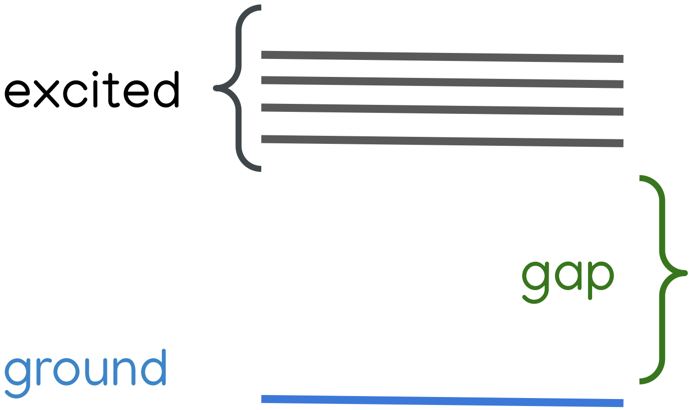

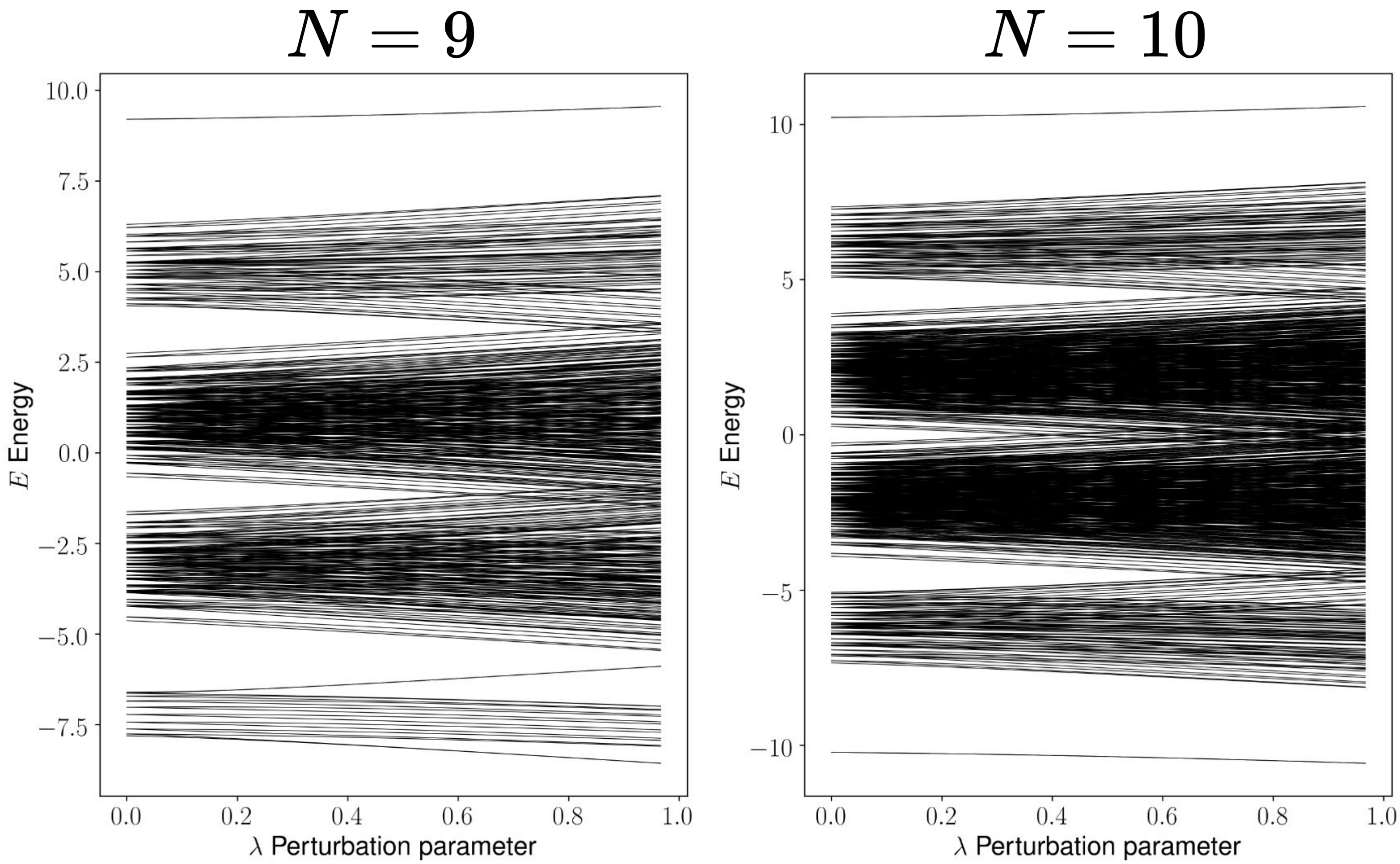

$N = 9$
$N = 10$
10.0
7.5
5.0
2.5
0.0
−2.5
−5.0
−7.5
E Energy
10
5
0
−5
−10
0.0
0.2
0.4
0.6
0.8
1.0
λ Perturbation parameter

Consecuencias en el eco de Loschmidt

N impar

$$\mathcal{L}(t) = \left| \sum_n e^{-iE_n t} |c_n|^2 \right|^2$$

$$c_n = \langle n | g \rangle \, .$$

Presencia de frustración

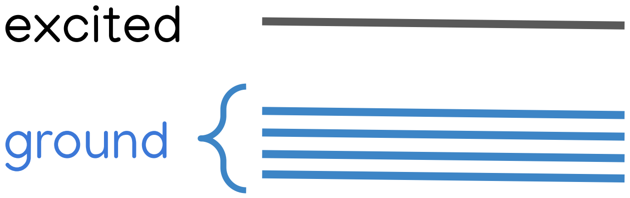

$$|c_0| \sim \sum_{i>0} |c_i|^2$$

N par

Ausencia de frustración

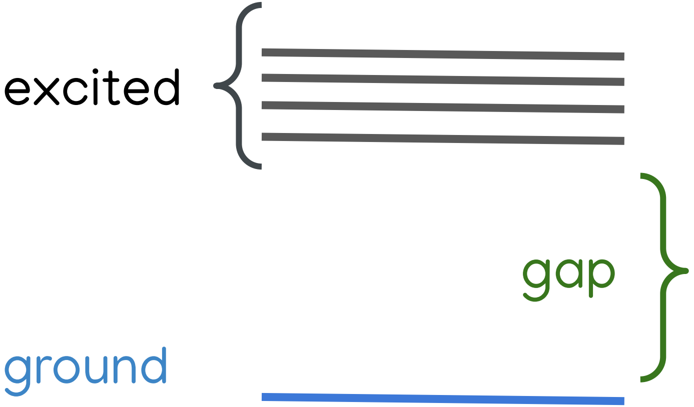

$$|c_0| \gg \sum_{i>0} |c_i|^2$$

04

Resultados

Sistema: Ising con campo transverso + impureza

$$H_1 = H_0 + \lambda\,\sigma_N^z \qquad H_0 = \sum_{j=1}^{N} \left(\sigma_j^x \sigma_{j+1}^x + h\sigma_j^z\right)$$

si $j = N \Rightarrow \sigma_N^x \cdot \sigma_1^x$

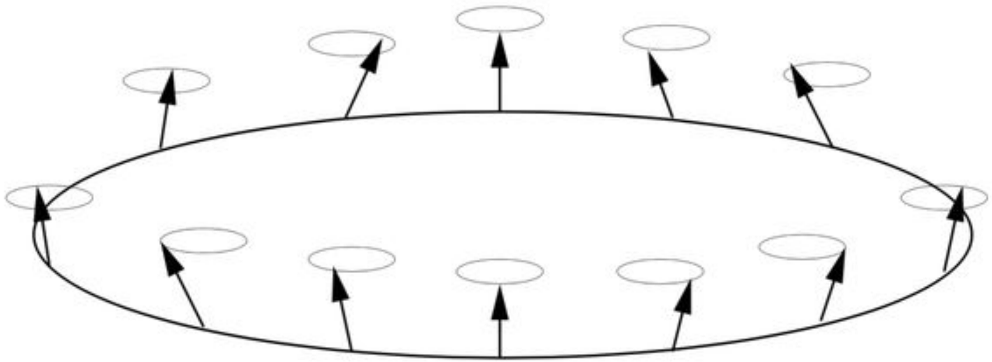

$h > 0$

Sistema: Ising con campo transverso con CC periódicas

Simetrías

$$H_0 = \sum_{j=1}^{N} \left(\sigma_j^x \sigma_{j+1}^x + h \sigma_j^z \right)$$

si $j = N \Rightarrow \sigma_N^x \cdot \sigma_1^x$

$\Pi^z = \bigotimes_{i=1}^{N} \sigma_i^z$ **Paridad**

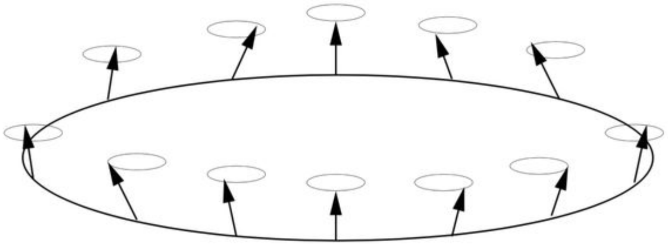

Traslación → **autoestados con momento bien definido**

$h > 0$

Sistema: Ising con campo transverso + impureza

$$H_1 = H_0 + \lambda \sigma_N^z \qquad H_0 = \sum_{j=1}^{N} \left(\sigma_j^x \sigma_{j+1}^x + h\sigma_j^z\right)$$

Rompe la simetría de traslación permitiendo que haya overlap entre los estados perturbados y toda la banda de menor energía (donde cada estado está caracterizado por un momento distinto)

Preserva la ruptura espontánea de simetría para mantener nulo el overlap con otros ground states.

Diferencias en el eco de Loschmidt

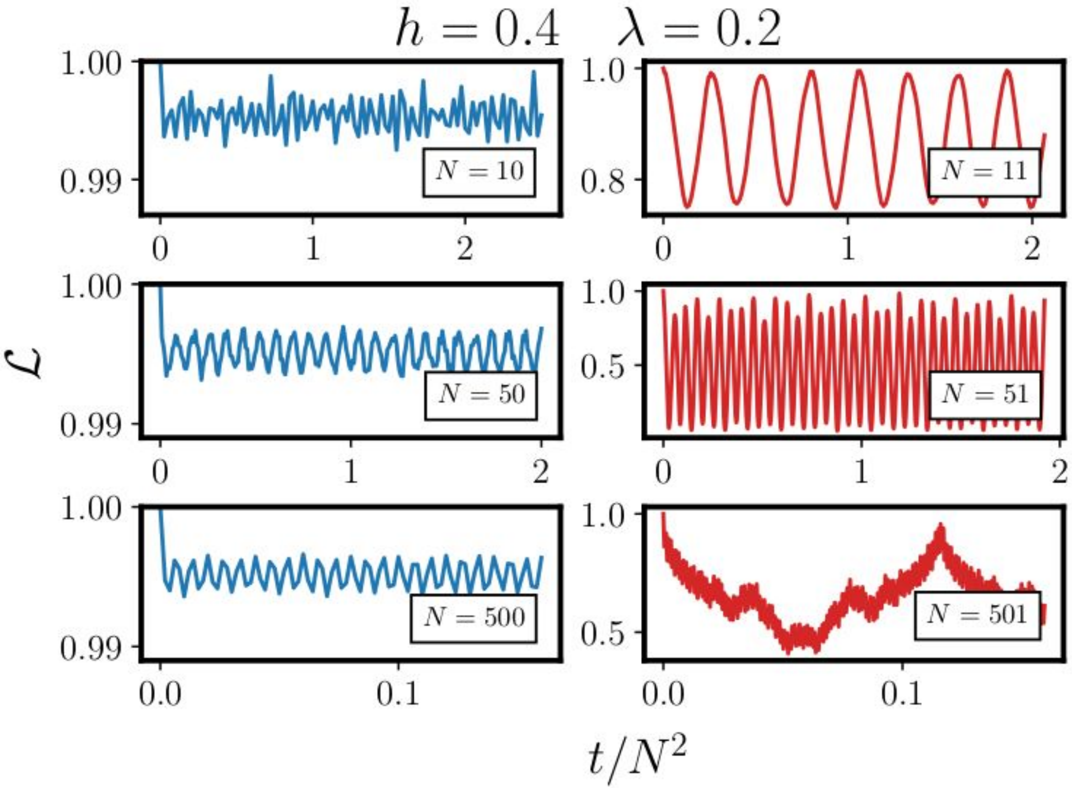

Diferencias en el eco de Loschmidt

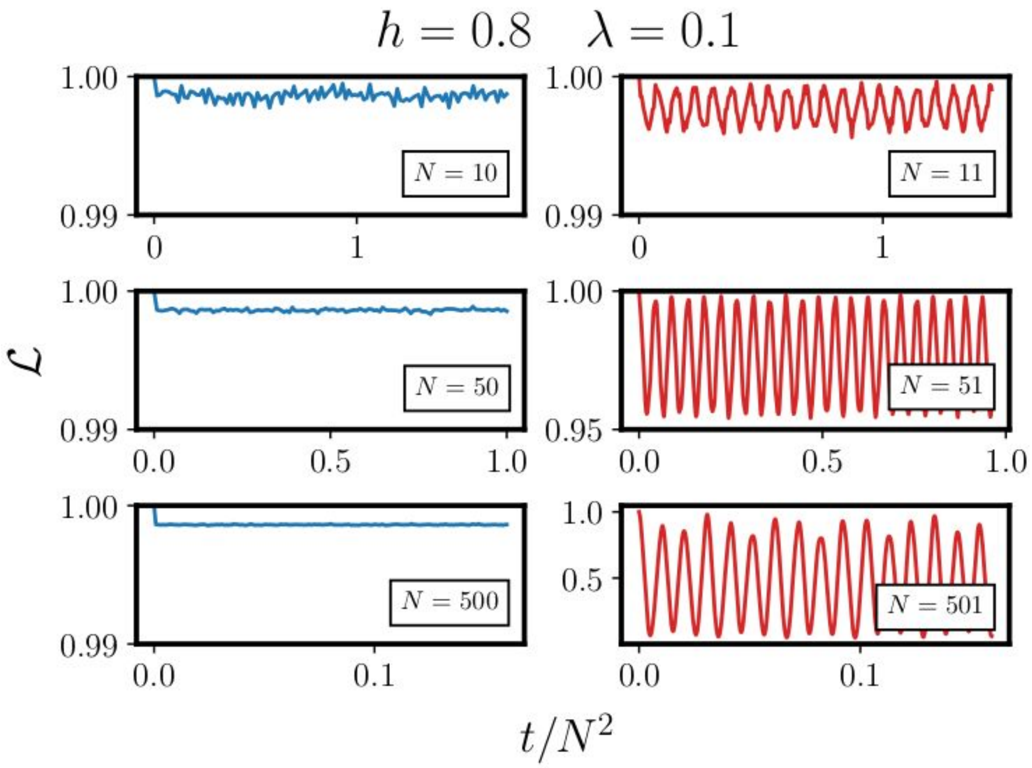

Diferencias en el eco de Loschmidt

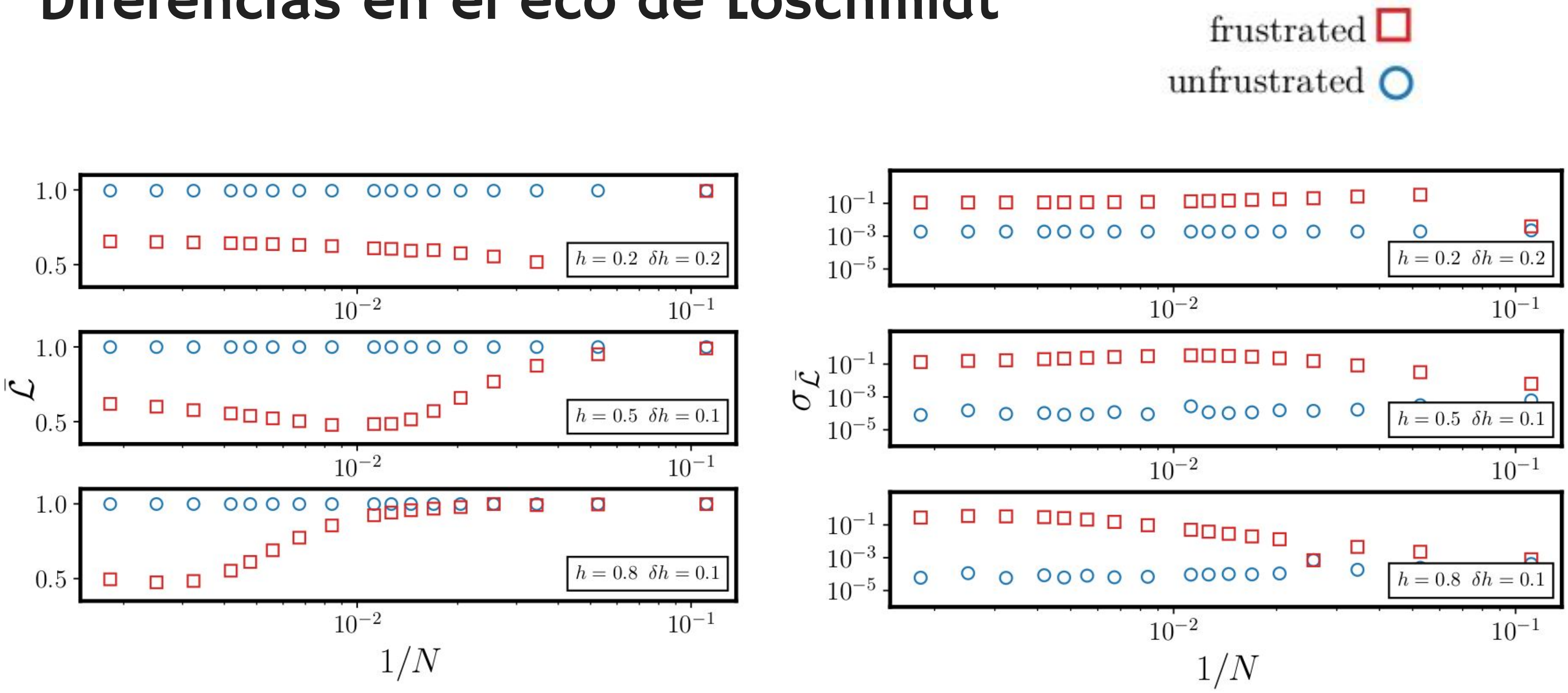

05

Conclusiones

Conclusiones

En cadena antiferro tipo Ising 1D con impureza (rompe simetría de traslación pero no de paridad) el eco de Loschmidt tiene distinto comportamiento para N par e impar

Este comportamiento se debe a los distintos espectros de energía resultandos de la presencia/ausencia de frustración topológica

El eco se puede medir experimentalmente a partir de la decoherencia de un sistema de dos niveles interactuando con el sistema de espines

Rossini, D., Calarco, T., Giovannetti, V., Montangero, S., & Fazio, R. (2007). Decoherence by engineered quantum baths. *Journal of Physics A: Mathematical and Theoretical*, *40*(28), 8033.

Ideas a futuro

- Probar si este efecto persiste para estados exitados

- Estudiar caos y OTOCs para este sistema

Muchas gracias

Periodically-driven quantum thermal machines from warming up to limit cycle

Junjie Liu,[1] Kenneth A. Jung,[2] and Dvira Segal[1,3]

[1]*Department of Chemistry and Centre for Quantum Information and Quantum Control, University of Toronto, 80 Saint George St., Toronto, Ontario, M5S 3H6, Canada*

[2]*Department of Chemistry, Stanford University, Stanford, California, 94305, USA*

[3]*Department of Physics, 60 Saint George St., University of Toronto, Toronto, Ontario, M5S 1A7, Canada*

(Dated: June 22, 2021)

Theoretical treatments of periodically-driven quantum thermal machines (PD-QTMs) are largely focused on the limit-cycle stage of operation characterized by a periodic state of the system. Yet, this regime is not immediately accessible for experimental verification. Here, we present a general thermodynamic framework that can handle the performance of PD-QTMs both before and during the limit-cycle stage of operation. It is achieved by observing that periodicity may break down at the ensemble average level, even in the limit-cycle phase. With this observation, and using conventional thermodynamic expressions for work and heat, we find that a complete description of the first law of thermodynamics for PD-QTMs requires a new contribution, which vanishes *only* in the limit-cycle phase under rather weak system-bath couplings. Significantly, this contribution is substantial at strong couplings *even at limit cycle*, thus largely affecting the behavior of the thermodynamic efficiency. We demonstrate our framework by simulating a quantum Otto engine building upon a driven resonant level model. Our results provide new insights towards a complete description of PD-QTMs, from turn-on to the limit-cycle stage and, particularly, shed light on the development of quantum thermodynamics at strong coupling.

A scalable helium gas cooling system for trapped-ion applications

F. R. Lebrun-Gallagher,[1] N. Johnson,[1] M. Akhtar,[1,2] S. Weidt,[1,2] D. Bretaud,[1,3] S. J. Hile,[1] A. Owens,[1] and W. K. Hensinger[1,2,a)]

[1)] *Sussex Centre for Quantum Technologies, University of Sussex, Brighton, BN1 9RH, U.K.*

[2)] *Universal Quantum Ltd, Brighton, BN1 6SB, U.K.*

[3)] *QOLS, Blackett Laboratory, Imperial College London, London, SW7 2BW, U.K.*

(Dated: 15 June 2021)

Microfabricated ion-trap devices offer a promising pathway towards scalable quantum computing. Research efforts have begun to focus on the engineering challenges associated with developing large-scale ion-trap arrays and networks. However, increasing the size of the array and integrating on-chip electronics can drastically increase the power dissipation within the ion-trap chips. This leads to an increase in the operating temperature of the ion-trap and limits the device performance. Therefore, effective thermal management is an essential consideration for any large-scale architecture. Presented here is the development of a modular cooling system designed for use with multiple ion-trapping experiments simultaneously. The system includes an extensible cryostat that permits scaling of the cooling power to meet the demands of a large network. Following experimental testing on two independent ion-trap experiments, the cooling system is expected to deliver a net cooling power of 111 W at $\sim$70 K to up to four experiments. The cooling system is a step towards meeting the practical challenges of operating large-scale quantum computers with many qubits.

Finite-time performance of a single-ion quantum Otto engine

Suman Chand,* Shubhrangshu Dasgupta, and Asoka Biswas
Department of Physics, Indian Institute of Technology Ropar, Rupnagar, Punjab 140001, India

We study how a quantum heat engine based on a single trapped ion performs in finite time. The always-on thermal environment acts like the hot bath, while the motional degree of freedom of the ion plays the role of the effective cold bath. The hot isochoric stroke is implemented via the interaction of the ion with its hot environment, while a projective measurement of the internal state of the ion is performed as an equivalent to the cold isochoric stroke. The expansion and compression strokes are implemented via suitable change in applied magnetic field. We study in detail how the finite duration of each stroke affects the engine performance. We show that partial thermalization can in fact enhance the efficiency of the engine, due to the residual coherence, whereas faster expansion and compression strokes increase the inner friction and therefore reduce the efficiency.

Nonequilibrium Casimir effects of nonreciprocal surface waves

Chinmay Khandekar,[1,*] Siddharth Buddhiraju,[1] Paul R. Wilkinson,[2] James K. Gimzewski,[2] Alejandro W. Rodriguez,[3] Charles Chase,[4] and Shanhui Fan[1,†]

[1]*Department of Electrical Engineering, Stanford University, California 94305, USA*
[2]*Department of Chemistry and Biochemistry, University of California Los Angeles, Los Angeles, California 90095, USA*
[3]*Department of Electrical and Computer Engineering, Princeton University, Princeton, New Jersey 08544, United States*
[4]*UnLAB, Savannah, Georgia 31405, USA*

(Dated: June 22, 2021)

We show that an isotropic dipolar particle in the vicinity of a substrate made of nonreciprocal plasmonic materials can experience a lateral Casimir force and torque when the particle's temperature differs from that of the slab and the environment. We connect the existence of the lateral force to the asymmetric dispersion of nonreciprocal surface polaritons and the existence of the lateral torque to the spin-momentum locking of such surface waves. Using the formalism of fluctuational electrodynamics, we show that the features of lateral force and torque should be experimentally observable using a substrate of doped Indium Antimonide (InSb) placed in an external magnetic field, and for a variety of dielectric particles. Interestingly, we also find that the directions of the lateral force and the torque depend on the constituent materials of the particles, which suggests a sorting mechanism based on lateral nonequilibrium Casimir physics.

Decoherence scaling transition in the dynamics of quantum information scrambling

Federico D. Domínguez,[1] María Cristina Rodríguez,[1,2] Robin Kaiser,[3] Dieter Suter,[4] and Gonzalo A. Álvarez[1,2,5,*]

[1] *Centro Atómico Bariloche, CONICET, CNEA, S. C. de Bariloche, Argentina.*
[2] *Instituto Balseiro, CNEA, Universidad Nacional de Cuyo, S. C. de Bariloche, Argentina.*
[3] *Université Côte d'Azur, CNRS, INPHYNI, F-06560, Valbonne, France.*
[4] *Fakultät Physik, Technische Universität Dortmund, D-44221, Dortmund, Germany.*
[5] *Instituto de Nanociencia y Nanotecnologia, CNEA, CONICET, S. C. de Bariloche, 8400, Argentina*

Reliable processing of quantum information for developing quantum technologies requires precise control of out-of-equilibrium many-body systems. This is a highly challenging task as the fragility of quantum states to external perturbations increases with the system-size. Here, we report on a series of experimental quantum simulations that quantify the sensitivity of a controlled Hamiltonian evolution to perturbations that drive the system away from the targeted evolution. Based on out-of-time ordered correlations, we demonstrate that the decay-rate of the process fidelity increases with the effective number K of correlated qubits as K^{α}. As a function of the perturbation strength, we observe a decoherence scaling transition of the exponent α between two distinct dynamical regimes. In the limiting case below the critical perturbation strength, the exponent α drops sharply below 1, and there is no inherent limit to the number of qubits that can be controlled. This resilient quantum feature of the controlled dynamics of quantum information is promising for reliable control of large quantum systems.

Cálculos

Resuelven el modelo mapeándolo primero a fermiones sin espín a través de la Transformación de Jordan-Wigner

Luego pasando al espacio de Fourier y allí aplicando una rotación de Bogoliubov que hace que el hamiltoniano sea diagonal

Para estudiar la perturbación utilizan teoría de perturbaciones para el caso degenerado

Franchini, F. (2017). *An introduction to integrable techniques for one-dimensional quantum systems*. Cham: Springer International Publishing.

Expresión analítica para el eco de Loschmidt

para $0 < h \ll \lambda \ll 1$

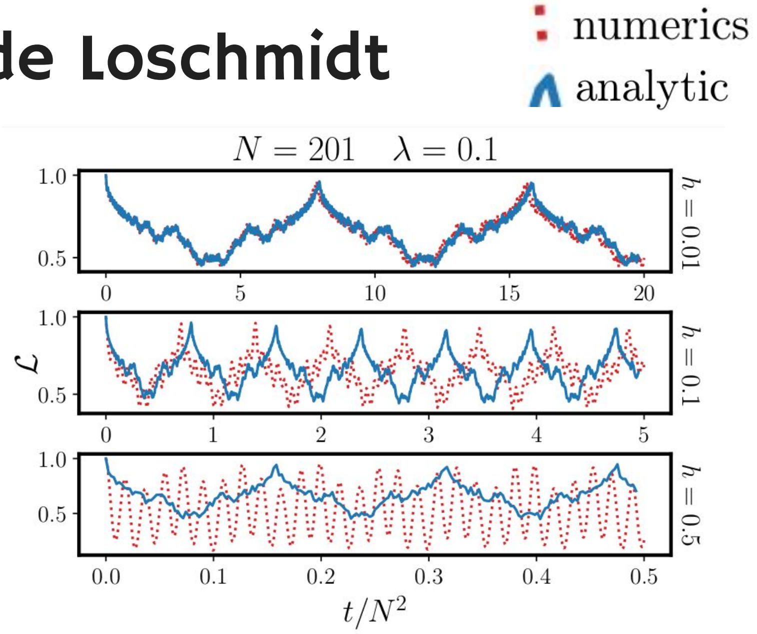

$\lambda\, \sigma_N^z$ **perturbación de 1er orden**

$h \sum_j \sigma_j^z$ **perturbación de 2do orden**

$$\mathcal{L}(t) = \left| \frac{2}{N(N-1)} \sum_{k=1}^{(N-1)/2} \tan^2\left[\frac{(2k-1)\pi}{2(N-1)}\right] \exp\left\{ -\imath 2ht \cos\left[\frac{(2k-1)\pi}{N-1}\right]\right\} + \frac{2}{N} \exp\left[\imath t(\lambda + h)\right] \right|^2 .$$

Límite termodinámico: dinámica fractal

$$\mathcal{L}(t) = \left| \frac{2}{N(N-1)} \sum_{k=1}^{(N-1)/2} \tan^2\left[\frac{(2k-1)\pi}{2(N-1)}\right] \exp\left\{-\imath 2ht \cos\left[\frac{(2k-1)\pi}{N-1}\right]\right\} + \underbrace{\frac{2}{N} \exp\left[\imath t(\lambda+h)\right]}_{\approx 0} \right|^2.$$

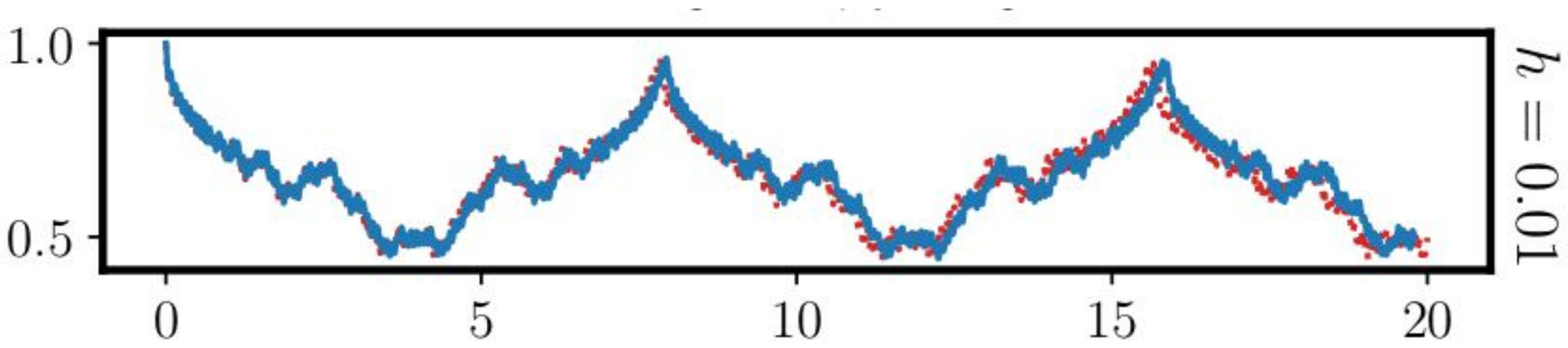

continua en todos lados, derivable en ningún lado

Límite termodinámico: dinámica fractal

$$W(x) = \sum_{n=0}^{\infty} a^n \cos(b^n \pi x), \quad 0 < a < 1$$

$$ab > 1$$

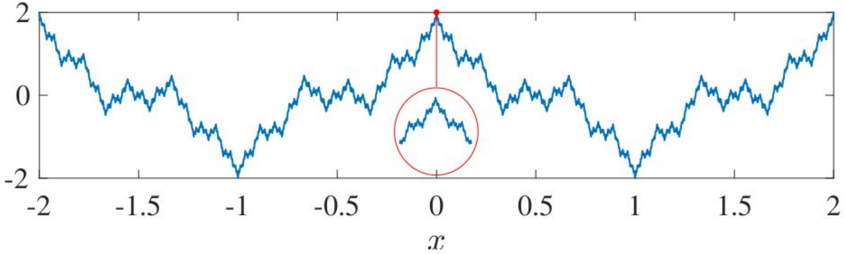

$$\mathcal{L}(t) \simeq \mathcal{F}\left(\frac{2ht}{N^2}\right)$$

$$\mathcal{F}(x) = \lim_{M\to\infty} \left| \frac{1}{2M^2} \sum_{k=1}^{M} \tan^2\left[\frac{(2k-1)\pi}{4M}\right] \times \right.$$

$$\left. \times \exp\left\{ -ix(2M+1)^2 \cos\left[\frac{(2k-1)\pi}{2M}\right]\right\} \right|^2$$